Evaluating empirical regression equations for *Vs* and estimating *Vs*30 in northeastern Taiwan

Chun-Hsiang Kuo [a,*], Kuo-Liang Wen [a,b], Hung-Hao Hsieh [a], Tao-Ming Chang [a], Che-Min Lin [a], Chun-Te Chen [b]

[a] National Center for Research on Earthquake Engineering, Taipei, Taiwan
[b] Institute of Geophysics, National Central University, Taoyuan, Taiwan

ABSTRACT

The shear wave velocity of shallow sediments is very important in seismic wave amplification and thus *Vs*30 is a well-known parameter for site classification. Based on the relationship between *Vs* and soil indexes, the empirical regression equations were evaluated using more than 600 data sets from the Ilan area and the Taipei Basin. Multivariable analysis, which can increase the accuracy of regression equations, was used in this study. Three extrapolations were compared, and then the most accurate bottom-constant extrapolation was adopted to estimate *Vs*30 at 16 boreholes, none of which reached a depth of 30 m. Ultimately *Vs*30 was derived for 110 free-field strong motion stations, and the stations in northeastern Taiwan were reclassified according to the *Vs*30-based NEHRP provisions. Regression equations of *Vs* and the extrapolation of *Vs*30 were also applied to boreholes with only *N*-values and corresponding depths of less than 30 m for assessing the *Vs*30 and NEHRP class.

Crown Copyright © 2010 Published by Elsevier Ltd. All rights reserved.

1. Introduction

It has been recognized that soft and young sediments covering firm bedrock can amplify seismic waves and cause severe damage during a large earthquake. Anderson et al. [1] noted that the strata in the top 30 m have a considerable influence on the character of the ground motions created. The NEHRP (see Table 1, the abbreviations and acronyms used in the present paper were tabulated as well as the original definitions) recommended *Vs*30 as a significant indicator for classifying sites in recent building codes [2,3]. The *Vs*30-based NEHRP Provision classes are shown in Table 2. Recently, Massa et al. [4] regarded site classification as a significant factor as well as magnitude and epicentral distance in the empirical strong-motion prediction equation. In addition, the NGA project [5,6] also suggested that the site conditions of recording stations are a significant parameter in strong ground motion prediction. It should be noted that strong motion records in Taiwan are also included in the PEER database.

Several researches recognized that *Vs* is correlated with soil indexes such as SPT-N (or N), depth, soil type, and geological epoch [7–9]. Adopting an approach akin to those mentioned above may be beneficial for the boreholes drilled previously, as they usually only have data pertaining to *N* and the corresponding depths, but without any measured *Vs*.

Since *Vs*30 is considered an important factor in ground motion prediction, assessing its value is essential. Seismic refraction, reflection, and SASW are all well-known noninvasive and active source techniques for estimating *Vs*. For example, Williams et al. [10] used high-resolution seismic refraction and reflection methods to derive *Vs* profiles as well as *Vs*30 in the St. Louis region. On the other hand, down-hole, up-hole, cross-hole, and suspension PS-logging are prevalent invasive and active source techniques. For example, Bang and Kim [11] used the SPT-up-hole method to determine *Vs* profiles to compare them with those determined by down-hole and SASW methods. Furthermore, passive source techniques such as the microtremor array method is also becoming popular [12,13]. Kuo et al. [13] estimated *Vs* profiles by three different techniques in shallow subsurface layers, and considered the suspension PS-logging as being able to observe precise P- and S-wave velocities in one-dimensional borehole measurements. Boore and Asten [14] compared shear-wave slowness profiles obtained by various invasive and noninvasive methods at several sites in the Santa Clara Valley. Ohta and Goto [15] proposed an in-situ down-hole technique for estimating *Vs* during a standard penetration test, and then combined it with other soil indexes to evaluate empirical regression equations.

Considering the fact that many boreholes drilled in the past did not reach 30 m, Boore [16] proposed an extrapolation using the correlation between *Vs*30 and the average *Vs* of other shallower depths. Boore and Joyner [17] and Huang et al. [18] were of the opinion that S-wave travel time increases with the depth in a

Table 1
The abbreviations and acronyms as well as the original definition used in the present study.

Abbreviations or acronyms	Original definitions
NEHRP	National Earthquake Hazard Reduction Program
Vs30	Average shear wave velocity of the top 30 m
NGA	Next Generation of ground motion Attenuation models
PEER	Pacific Earthquake Engineering Research Center
Vs	Shear wave velocity
SPT-N or N	Blow number of the Standard Penetration Test
SASW	Spectra analysis of surface wave
CWB	Central Weather Bureau
NCREE	National Center for Research on Earthquake Engineering
USCS	Unified Soil Classification System
SC, SP, SM, SW, CL, ML, CH, and MH	The first letter means the major compositions, here are sand (S), clay (C), and mud (M); the second one means either the characteristics or minor composition, here are clay (C), poorly graded (P), mud (M), well-graded (W), low-plasticity (L), and high-plasticity (H)
TAP and ILA	The code of strong motion stations in Taipei and Ilan
DH and SH	Deep boreholes ($\geqq$30 m) and Shallow boreholes ($<$30 m)
D	Depth
LSS	Least-square of single station
STS	Statistical extrapolation
BCV	Bottom constant velocity
Ss	Shear wave slowness

Table 2
NEHRP site definition in terms of Vs30 and simple geological descriptions.

NEHRP site class	Description	Range of Vs30 (m/s)
A	Hard rock	$Vs30 > 1500$
B	Firm to hard rock	$1500 \geq Vs30 > 760$
C	Dense soil and soft rock	$760 \geq Vs30 > 360$
D	Stiff soil	$360 \geq Vs30 \geq 180$
E	Soft soil	$180 > Vs30$

power-law form, and thus Vs30 can be calculated by a least-square fit at each single borehole which does not reach 30 m. Boore [16] and Kuo et al. [13] set the deepest velocity as a constant in the ensuing depths to 30 m for the shallow boreholes. For boreholes that only have N and the corresponding depths, we used empirical regression equations to estimate their Vs; for those that were not drilled to 30 m, an extrapolation approach was adopted to assess their Vs30. Thus in this study we implemented two techniques: empirical Vs equations and extrapolations for Vs30. These methods are useful for estimating the Vs profiles of ancient boreholes that only have N and/or do not extend to 30 m. In addition, both techniques have the advantages of being convenient, efficient, and economical, making them well suited for the NEHRP.

2. Database and local geology

In Taiwan, the CWB and the NCREE have been establishing a free-field strong-motion station drilling project to construct an engineering geological database for free-field strong-motion stations and for measuring the P- and S-wave velocities using a suspension PS-logging system since 2000. The physical characteristics of layers, such as density and grain size are being measured from the core samples; SPT-N values are obtained by in-situ measurement, and soils are classified according to the USCS. The time resolution of the suspension PS-logging measurement is

0.001 s and the frequency of the velocity measurement is 0.5 or 1 m per point. The drilled depths in this project must exceed at least 35 m to ensure that Vs30 is able to be measured by a PS-logging system; moreover, several boreholes were drilled over 50 m and several were drilled over 100 m according to the annual contract stipulations. However, some boreholes drilled in the first or second year do not reach the required 30 m.

In this study, 641 and 719 data sets (until 2008) were used to develop empirical equations in the Ilan area and the Taipei Basin, respectively. Specimens with N smaller than 50 as well as a depth smaller than or equal to 50 m were selected to evaluate the regression equations. Soil type is considered an important factor in a Vs regression equation, therefore SC, SP, SM, and SW were categorized as "sand"; CL, ML, CH, and MH as "clay and silt". Afterwards, we select sites at which boreholes extend to 30 m to examine three extrapolations [13,16,18]. For this purpose, 56 and 38 sites were used in Taipei and Ilan, respectively. The boreholes locate at strong motion stations in Taipei (Ilan) with depths of more than 30 m were named TAP-DH (ILA-DH); on the other hand, those with depths of less than 30 m were tagged TAP-SH (ILA-SH). Fig. 1 shows frequency distribution of depth of the 110 boreholes in Taipei and Ilan; 94 of the 110 boreholes are greater than 30 m.

Four Quaternary sedimentary formations covered on the Tertiary basement of the Taipei Basin, which are Sungshan, Chingmei, Wuku, and Banchiao Formations from top to bottom. The thickness of sediments was indicated by Wang et al. [19], as well as the average seismic velocities of layers. The Vs of Sungshan and Chingmei formations obtained by seismic reflections are about 170–340 and 450 m/s, respectively; the basement depths, otherwise, are greater than 600 m at the northwest and could shallow than 50 m around the basin edge [19]. The thickness of sediments in the Ilan Basin was illustrated by Chiang [20]. He indicated two sediment strata, which were formed in Holocene and Pleistocene, cover on the Tertiary bedrocks, as well as the P-wave velocities are 500–1600, 1800–2000 and 3300 m/s, respectively. The thickness of sediments was greater than 1400 m near the middle coast and became shallower than 100 m around the basin edge. Kuo et al. [13] conducted seven microtremor arrays in the Ilan Basin and the estimated Vs were almost all lower than 400 m/s at the depth smaller than 50 m.
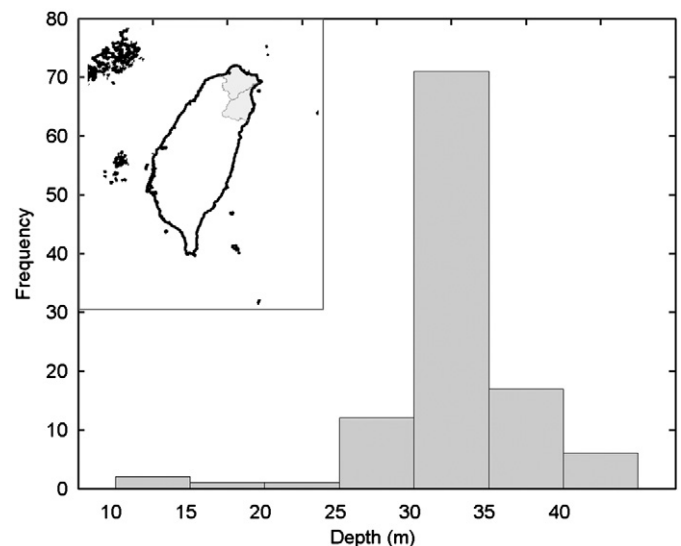
Fig. 1. Histogram for depth distribution of the 110 boreholes in Taipei and Ilan. The districts of Taipei (the north gray area) and Ilan (the south gray area) were sketched in the small scheme.

3. Empirical equations of shear wave velocity

3.1. Previous empirical equations

Many researchers have evaluated empirical equations of shear wave velocity for their efficiency and economy. Thirteen representative studies are shown in Table 3. Ohta and Goto [7,15] measured Vs during a Standard Penetration Test and then evaluated the empirical equations in terms of soil indexes. Their study first proposed a technique of multivariable analysis in Vs empirical equations. The research by Hamilton [21] and Holzer et al. [22] yielded the depth-dependent regression equations. As is evident from Table 3, some equations are only related to N. This is the case in the studies by Ohsaki and Iwasaki [23], Imai [24], Seed and Idriss [25], Pitilakis et al. [26], Hasancebi and Ulusay [27], Sykora and Stokoe [28], and Lee and Tsai [29].

However, Ohta and Goto [7], Lee [8], Chen et al. [9], and Chapman et al. [30] considered both depth and N in their empirical equations (depth information of Chapman's equations was involved in the effective overburden pressure (σ_v)), and therefore they introduced a multiple regression analysis. Lee [8] further discussed the multicollinearity problem caused by the high correlation among independent variables during multivariable analysis. Lee and Tsai [29] used the same data (but only until 2005) as the present study to establish the spatial relationship between Vs and N. In our research the corrected N_1 became worse in its correlation with Vs. This phenomenon was also mentioned by Lee and Tsai [29], and thus overburden-correction was not used in this study. For the rest, energy of SPT was not measured in the data sets. Some might argue that N and D are coupled because the overburden-correction was not carried out. However, when we adopted the multivariable regression, two examinations were being considered (and are described in the following section) to avoid the multicollinearity problem caused by two or more highly correlated independent variables. In other words, the multivariable regression can avoid the coupling effect between N and D.

3.2. Regression of the empirical equations

Most researchers hypothesized Vs as being in a power-law relationship with N or with the depth (Table 3). However, in this study we suggested that the regression model must be decided by the maximum correlation coefficient (R) between Vs and N or depth. Furthermore, the multivariable analysis was carried out to evaluate the regression equations unless the data could not pass either of the following two examinations. (1) rule of thumb test, in which statisticians usually suggest R between any two independent variables should be smaller than 0.7 [31]. (2) Stepwise selection: This procedure is a combination of backward and forward approaches and thus the criteria we set were that the probability of F had to be statistically lower than 0.05 for entry and higher than 0.1 for removal [32]. The variables were examined by these two criteria to avoid multicollinearity. Soil types (sand and clay & silt) and geological epoch were also considered in the process of regression if they could increase R of the evaluated equations. Subsequently, the empirical equation for the Ilan area for all soils was evaluated as

$$Vs = 169.04 + 4.46N + 0.59D \qquad (1)$$

It has the largest R (0.710), exhibits the best empirical equation in the Ilan area, and is a linear type. The standard error of this equation is 43.54. Both independent variables are involved in

Table 3
The representative empirical equations of shear wave velocity quoted in this study. The unit of Vs is meters per second.

Author	Regression equation	Soil type	Samples
Ohsaki and Iwasaki [23]	$Vs = 82N^{0.39}$	All	220
Hamilton [21]	$Vs = 128D^{0.28}$	Mud	29 sites
Imai [24]	$Vs = 91N^{0.337}$ $Vs = 80.6N^{0.331}$ $Vs = 102N^{0.292}$	All Sand Clay	943 151 183
Ohta and Goto [7]	$Vs = 62.14N^{0.219}D^{0.23} \times 1.000$ $Vs = 62.14N^{0.219}D^{0.23} \times 1.091$ $Vs = 62.14N^{0.219}D^{0.23} \times 1.029$ $Vs = 62.14N^{0.219}D^{0.23} \times 1.073$ $Vs = 62.14N^{0.219}D^{0.23} \times 1.151$	Clay Fine sand Medium sand Coarse sand Sand & gravel	300
Seed and Idriss [25]	$Vs = 61N^{0.5}$	All	–
Sykora and Stokoe [28]	$Vs = 100.5N^{0.29}$	Sand	–
Lee [8]	$Vs = 71.9(D+1)^{0.39}$ $Vs = 86.1N^{0.116}(D+1)^{0.244}$ $Vs = 82.8N^{0.134}(D+1)^{0.233}$ $Vs = 84.5N^{0.118}(D+1)^{0.246}$	SM CL ML CL/ML	126 265 100 365
Pitilakis et al. [26]	$Vs = 145(N_{60})^{0.178}$ $Vs = 132(N_{60})^{0.271}$	Sand Clay	15 sites
Chen et al. [9]	$Vs = 163.59 + 4.09D + 2.2(N_1 - N_{1,avg})$	All	45 sites
Holzer et al. [22]	$Vs = 75.2 + 3.99D$	Mud	135
Chapman et al. [30]	$Vs = 85.13N^{0.153}\sigma_v^{0.147}$ $Vs = 92.25N^{0.266}\sigma_v^{0.072}$	Sand Clay	223 154
Hasancebi and Ulusay [27]	$Vs = 90N^{0.309}$ $Vs = 90.8N^{0.319}$ $Vs = 97.9N^{0.269}$	All Sand Clay	97
Lee and Tsai [29]	$Vs = 137.153N^{0.229}$ $Vs = 98.07N^{0.305}$ $Vs = 163.15N^{0.192}$	All Sand Silt and clay	28 sites 15 sites 15 sites

Eq. (1) and are irrelevant to soil type and geological epoch. However, considering the geological epoch and the soil type resulted in increasing R in the Taipei Basin. The boreholes in the Taipei Basin were selected such to ensure that the data sets are all in the identical geological epoch (Holocene), and the elected data were grouped into two soil types, that is to say, sandy soils and clayey & silty soils. Afterwards, the multiple regression equations of the Taipei Basin were evaluated as

$$Vs = 93.11N^{0.242}D^{0.136} \text{ for sand} \tag{2}$$

$$Vs = 114.55N^{0.168}D^{0.143} \text{ for clay and silt} \tag{3}$$

Eqs. (2) and (3) have the largest R, 0.671 and 0.685, as well as the standard errors, 74.78 and 56.66, respectively. Eqs. (1)–(3) were plotted three dimensionally together with the data sets in Fig. 2.

4. Extrapolations of *Vs*30

4.1. Methodology

Boore [16] found that numerous measurements of near-surface Vs do not reach 30 m, such as the boreholes at the K-NET stations in Japan, which are between 10 and 20 m; in a recent compilation in California [33] more than half the boreholes (142 of 277) are lower than 30 m, and 193 of 202 seismic cone penetrometer measurements in the Oakland-Alameda area of California [22,34] are less than 30 m. Therefore, he found that plots of log Vs30 against log $Vs(d)$ for a series of assumed depths d could be fitted by a straight line by using boreholes with actual depths reaching or exceeding 30 m. $Vs(d)$ is the time-averaged velocity from the top to a depth d. Based on this, a power-law relation between Vs30 and $Vs(d)$ was assumed and the equation was given as

$$\log Vs30 = a + b\log Vs(d) \tag{4}$$

The coefficients (a and b) were obtained in various depths (usually from 10 to 28 m). In Taiwan, Lee et al. [35] researched surface geology, response spectra and horizontal to vertical spectral ratios and classified 708 free-field strong motion station sites into four categories; i.e., classes B–E. Huang et al. [18] classified 87 free-field strong motion stations in central Taiwan based on Vs30 criteria, 85 of which were previously classified by Lee et al. [35]. However, Huang et al. [18] reclassified 65 of these 85 sites different than Lee et al. [35]. For the boreholes were not drilled to 30 m, Huang et al. [18] assumed that the S-wave travel time increased with the depth in a power-law form; therefore, they calculated Vs30 using the least-square method in each single well that did not reach 30 m. Kuo et al. [13] set the deepest velocity as a constant in the ensuing depths to 30 m, and then estimated Vs30 in order to compare them with the Vs profiles estimated by other methods in Ilan.

Sokolov et al. [36] analyzed the site effect on class B sites in Taiwan based on the classification of Lee et al. [35] and indicated that station TAP051 has a specific amplification on the fundamental frequency of 6.5–8 Hz. They believed that this peculiarity was caused by a thin (10–12 m) layer of soft soil ($Vs=250–320$ m/s). It also seemed to indicate that the earlier classification might contain some mistakes. That is why Lee and Tsai [29] revised their previous classification by using velocity data (until 2005) of 230 strong-motion boreholes as well as 4885 engineering boreholes. For examining their new classification in Ilan and Taipei, This study used the latest (until 2008) data. Three extrapolations named the least-square of single station (LSS) [17,18], bottom constant velocity (BCV) [13,16], and statistical extrapolation (STS) [16,37] were also examined using ILA-DH and TAP-DH in the following section.

4.2. Comparison of the three extrapolations

ILA-DH includes 38 boreholes, TAP-DH includes 56 boreholes, ILA-SH includes seven boreholes, and TAP-SH includes nine boreholes. Thus, 110 strong motion stations were drilled in northeastern Taiwan. ILA-DH and TAP-DH were used to examine the accuracy of three extrapolations (Table 4 and Fig. 3). Figs. 3a and b illustrate the estimated Vs30 values (*y*-axis) by the three extrapolations versus the real Vs30 values (*x*-axis) obtained by PS-logging in Ilan and Taipei, respectively. The assumed depths were 15, 20, and 25 m from left to right. By defining an error
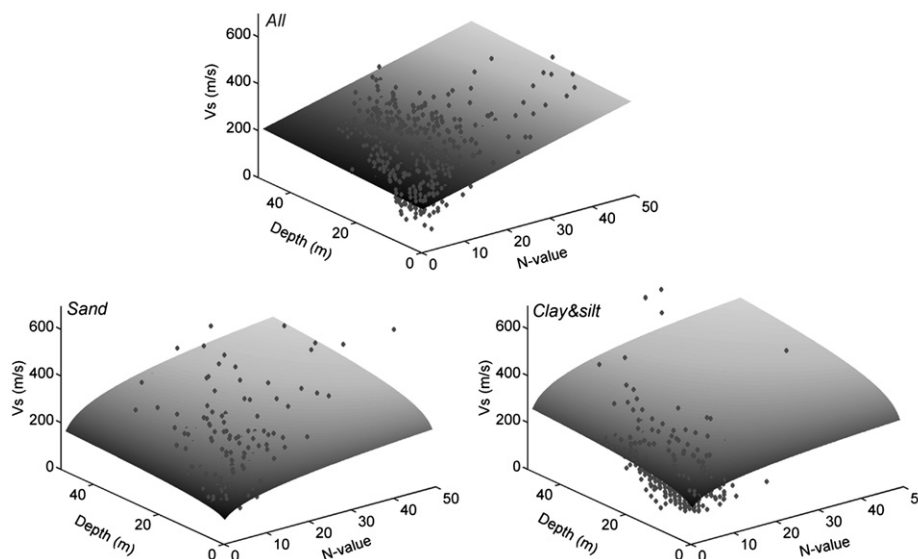

Fig. 2. Three-dimensional diagrams of regression equations and data sets for Ilan and the Taipei Basin. The upper plane is Eq. (1), the lower left curved surface is Eq. (2), and the lower right one is Eq. (3). The dots are data sets.

Table 4
The Err% obtained from three extrapolations in Ilan and Taipei at three assumed depths. The percentages behind " $\pm$ " are the standard deviations.

Assumed depth (m)	Ilan			Taipei		
	LSS	STS	BCV	LSS	STS	BCV
15	10.17% $\pm$ 7.16%	11.30% $\pm$ 6.77%	4.72% $\pm$ 3.14%	13.89% $\pm$ 9.47%	11.10% $\pm$ 7.82%	9.43% $\pm$ 7.38%
20	7.29% $\pm$ 5.11%	6.70% $\pm$ 4.06%	2.72% $\pm$ 2.34%	10.10% $\pm$ 7.83%	7.14% $\pm$ 5.04%	3.70% $\pm$ 3.40%
25	5.09% $\pm$ 3.72%	2.99% $\pm$ 1.99%	1.08% $\pm$ 1.15%	7.47% $\pm$ 5.80%	3.24% $\pm$ 2.47%	1.42% $\pm$ 1.73%
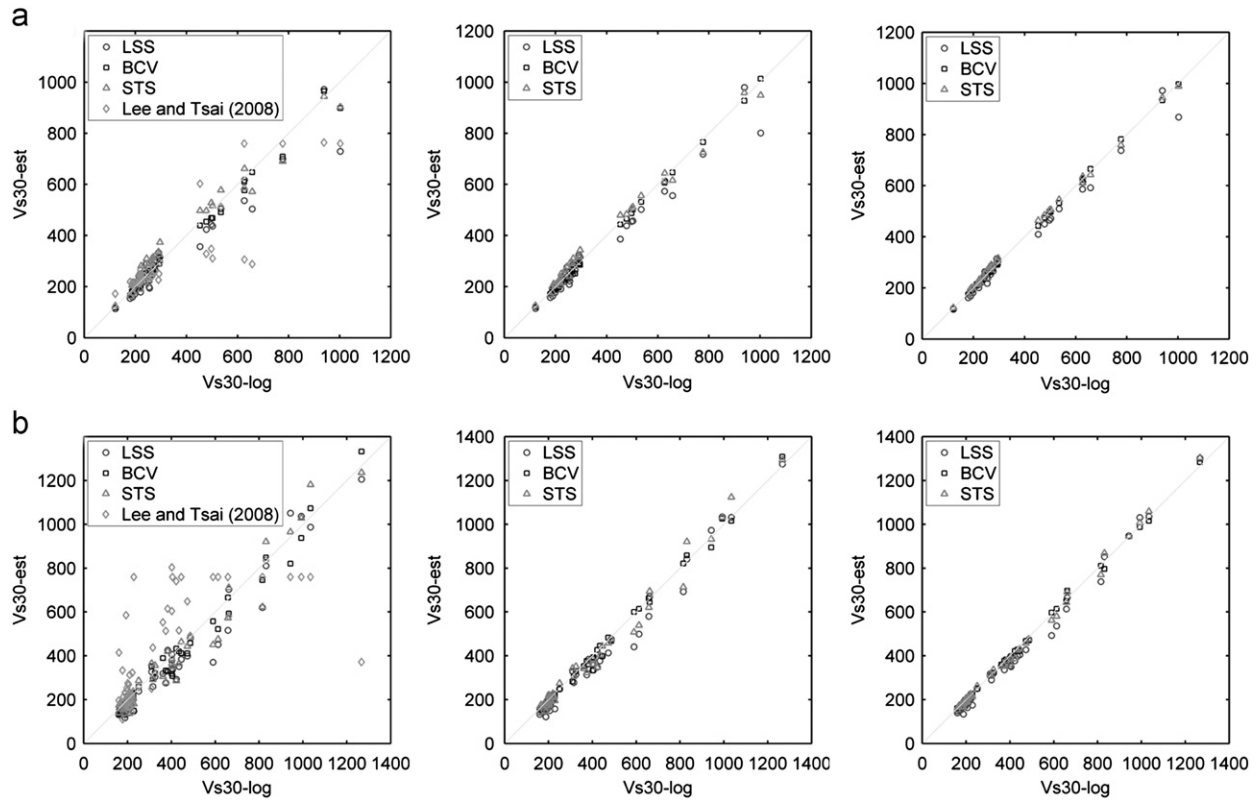
Fig. 3. Estimated Vs30 (y-axis) by three extrapolations versus real Vs30 (x-axis) observed by PS-logging in (a) Ilan and (b) Taipei. Assumed depths from left to right are 15, 20, and 25 m. Open circle, square, and triangle indicate the estimated Vs30 by LSS, BCV and STS extrapolations, respectively. In the left two diagrams, open diamonds denote large divergences between the estimated [29] and real Vs30 values.

percentage (Err%):

$$Err\% = \frac{\sum |Vs - Ve|/Vs}{n} \times 100\% \qquad (5)$$

where Vs is the measured S-wave velocity by PS-logging, Ve is the estimated S-wave velocity by extrapolation, and n is the number of data, the accuracy of these three extrapolations was examined by this equation (Table 4). Surprisingly, the smallest Err% was obtained by BCV at all assumed depths, rather than by STS. The Err% in Table 4 all decrease as the assumed depths increase. Besides, both Fig. 3 and Table 4 show that LSS results in the largest error for estimating Vs30 at each depth.

4.3. Estimating Vs30 at boreholes shallower than 30 m

For ILA-SH and TAP-SH, we applied the three extrapolations as mentioned above to estimate the values of Vs30 and their Vs30-based NEHRP class. The extrapolated Vs30 are shown in Table 5. Fortunately, the site classifications are identical except for using LSS; thus the results with the highest confidence are shown. Table 5 also indicates that LSS sometimes underestimates Vs30 and classifies sites into a softer class (ILA013, ILA054, and TAP057).

5. Discussions

Although empirical regression equations have advantages in terms of being convenient, efficient, and economical, there is a notable drawback. The maximum value of Eqs. (1)–(3) were 405.13, 379.24, and 358.24 (m/s) while N=49 and D=30. Therefore, the empirical regression equations could not be applied at the sites of A and B classes. This is because N is equal to or larger than 50 at the A and B class sites. However, those data were not used to evaluate the regression equations.

It is difficult to illustrate the three-dimensional curved surfaces together and compare them with each other; therefore, this study compared the Vs profiles obtained by PS-logging measurements with those estimated by different regression equations. Figs. 4a and b show the comparisons of the Vs profiles, which include the Vs obtained by PS-logging measurements, estimated by regression equations in this study, and previous equations. Fig. 4a shows the result at ILA005. It is obvious that the Vs profile from this study is nearly identical to that of Lee and Tsai [29]; and for the rest they are both similar to the PS-logging result. In addition, Fig. 4b plotted another example (TAP019) in the Taipei Basin. The regression equations of Lee [8] were evaluated using a different database in

the Taipei Basin. However, when compared with the actual Vs profile (PS-logging), the result of the present study is substantially more accurate than that of others. It should be noted that Lee and Tsai [29] used the same database as the one used in this study, but their data are only until 2005 and contain only 15 sites in the Taipei Basin; while 65 sites were employed in the present study. This is why our estimated Vs profile is better than that of Lee and Tsai [29] at TAP019.

The present study considered that some shallow boreholes (depth < 30 m) have only N; however, the Vs30 can still be obtained. The Vs is first derived by empirical regression equations, and Vs30 is then estimated by extrapolation. For example, two boreholes (DB-151, SS-B-09) which have no velocity data, were acquired from the website of the Central Geology Survey of Taiwan (http://210.69.81.69/geo/frame/gsb88.cfm). DB-151 is located in Ilan and has a depth of only 25 m. We utilized Eq. (1) to estimate the Vs profile in Fig. 5a as well as its Vs30 (238.91 m/s) by BCV. The other one is SS-B-09 which is located in the Taipei Basin and has a depth of 25.5 m. The

estimated Vs profile (by Eqs. (2) and (3)) is plotted in Fig. 5b, and the Vs30 via BCV is 211 m/s. They were both classified as class D. ILA035 and TAP012 are the nearest strong motion stations, respectively. The Vs30 were measured at 293.1 and 207.37 m/s by PS-logging, hence they were also classified into class D. This indicates that this approach can obtain reasonable results.

Since the comparison showed that BCV is more reliable than STS, we suspected that the Vs increases more gently with depth in northeastern Taiwan than in California [16]. We further compared the average Ss at the sites in northeastern Taiwan and California at four depths (5, 10, 20, and 30 m). Fig. 6 shows six representative average Ss in California [14] together with two average Ss (ILA and TAP stations) in northeastern Taiwan at depths of 5, 10, 20, and 30 m. The Ss of ILA and TAP stations are the average at four depths of ILA-DH and TAP-DH. Fig. 6 clearly shows that except for CCOC, the average Ss at other sites in California decreased more rapidly than at stations of ILA and TAP.

One of the objectives in this study was to reclassify the free-field strong motion stations in northeastern Taiwan. Table 6 shows the classification of 110 strong motion stations based on the Vs30 criteria of NEHRP provisions in Ilan and Taipei, as well as the classification of Lee and Tsai [29], in parentheses. As for the classification of ILA-SH and TAP-SH, the Vs30 were given by means of BCV. Thirty-five of the 110 stations were reclassified. Nine class B stations were reclassified as class C; 1 class B station was reclassified as class D; 2 class C stations were reclassified as class B; 3 class C stations were reclassified as class D; 1 class C station was reclassified as class E; 6 class D stations were reclassified as class C; 4 class D stations were reclassified as class E; and 9 class E stations were reclassified as class D. Finally, there are 14 stations in class B, 28 in class C, 60 in class D, and 8 in class E, which are denoted by diamonds, squares, triangles, and circles, respectively (Fig. 7). TAP051, which was referred by Sokolov et al. [36], was classified into class B by Lee et al. [35]; however, it was reclassified into class C2 (Vs between 490 and 620 m/s) by Lee and Tsai [29], but the measured Vs30 is only 401.82 m/s and should be classified into class C1 (Vs between 360 and 490 m/s) according to the criteria used in Lee and Tsai [29]. The site classification of Lee and Tsai [29] is much better than that of Lee et al. [35]; nevertheless, there might be some errors in the Vs30 values, and so we tried to quantify them in this study. The left two diagrams of Fig. 3 show large divergences between the real (x-axis) and the estimated Vs30 (y-axis) by Lee and
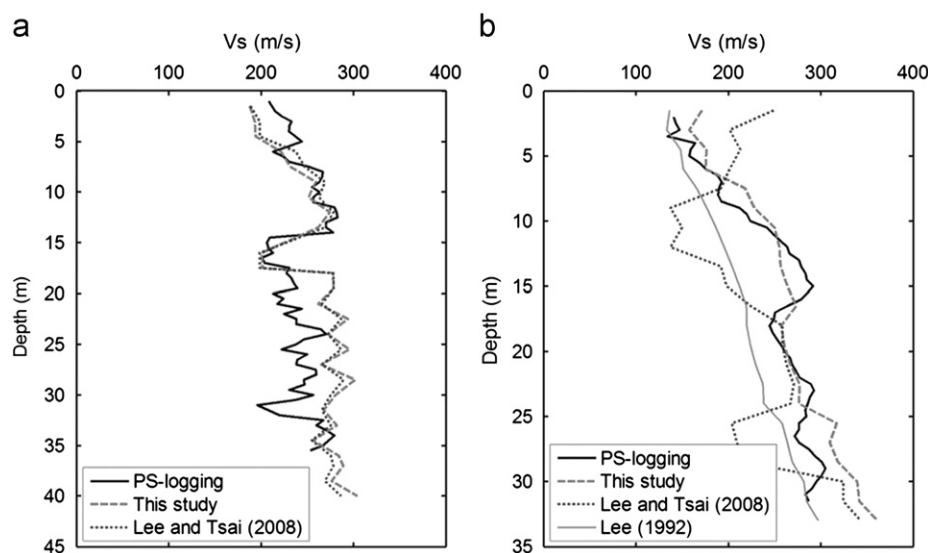
Table 5
Estimated Vs30 and site classification of ILA-SH and TAP-SH. Numbers and letters in the parentheses are borehole depths and site classification, respectively. The stars before Vs30 indicate this site class is different from that via the other two approaches.

Stations (depth < 30 m)	Vs30 (m/s)		
	LSS	BCV	STS
ILA013 (19 m)	*176.05 (E)	194.50 (D)	204.65 (D)
ILA014 (23 m)	291.17 (D)	307.46 (D)	322.17 (D)
ILA027 (11 m)	204.13 (D)	212.65 (D)	238.68 (D)
ILA044 (27 m)	143.78 (E)	159.00 (E)	156.80 (E)
ILA046 (28 m)	387.63 (C)	397.59 (C)	393.83 (C)
ILA049 (13 m)	192.68 (D)	187.12 (D)	202.32 (D)
ILA054 (28 m)	*717.58 (C)	783.09 (B)	771.41 (B)
TAP016 (27 m)	320.34 (D)	326.64 (D)	327.79 (D)
TAP040 (29 m)	395.44 (C)	432.53 (C)	431.10 (C)
TAP045 (27 m)	966.19 (B)	987.65 (B)	995.40 (B)
TAP046 (27 m)	829.15 (B)	822.03 (B)	819.03 (B)
TAP057 (28 m)	*320.42 (D)	366.57 (C)	361.41 (C)
TAP058 (27 m)	994.32 (B)	1056.71 (B)	1072.75 (B)
TAP059 (27 m)	395.24 (C)	450.55 (C)	441.57 (C)
TAP075 (26 m)	921.24 (B)	851.06 (B)	904.07 (B)
TAP094 (27 m)	412.98 (C)	409.86 (C)	417.35 (C)

Fig. 4. Both are comparisons of obtained and estimated Vs profiles at (a) ILA005 and (b) TAP019. Black thick line is Vs profiles obtained by PS-logging, gray dash line is estimated by empirical equations in this study, gray dotted line is estimated by equations of Lee and Tsai [29], and gray thin line is estimated by equations of Lee [8].
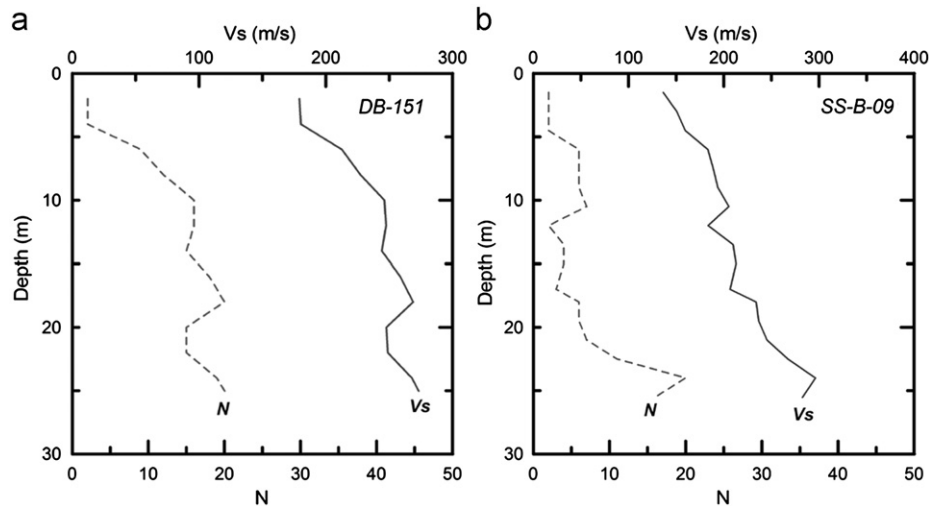
Fig. 5. N and estimated Vs profiles at (a) DB-151 and (b) SS-B-09 in Ilan and the Taipei Basin. Both sites are classified as class D.
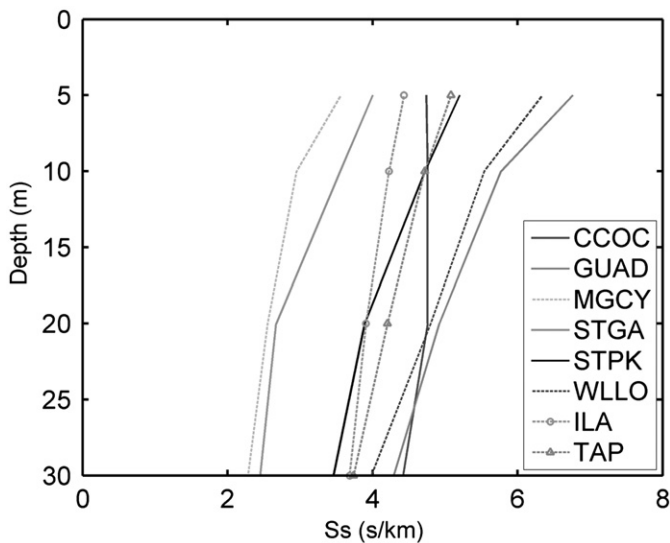

Fig. 6. CCOC, GUAD MGCY, STGA, STPK, and WLLO are six sites in California at four depths (5, 10, 20, and 30 m) [14]. ILA and TAP represent the average Ss of ILA-DH and TAP-DH at the same depths.

Table 6
Site classification of 110 stations base on the Vs30 criteria of NEHRP provisions. The classification of Lee and Tsai [29] were displayed in parentheses.

Station	Class	Station	Class	Station	Class	Station	Class
ILA001	B (B)	ILA039	D (D1)	TAP012	D (D1)	TAP052	C (C2)
ILA002	D (D2)	ILA040	D (D1)	TAP013	D (D1)	TAP054	D (D2)
ILA003	D (D1)	ILA041	D (E)	TAP014	D (E)	TAP056	C (B)
ILA004	E (E)	ILA042	D (D1)	TAP015	D (E)	TAP057	C (C1)
ILA005	D (D2)	ILA044	E (D1)	TAP016	D (C3)	TAP058	B (B)
ILA006	D (D2)	ILA046	C (D3)	TAP017	D (E)	TAP059	C (B)
ILA008	D (D1)	ILA048	D (D1)	TAP019	D (D1)	TAP065	B (B)
ILA012	D (D1)	ILA049	D (D1)	TAP020	D (E)	TAP066	C (B)
ILA013	D (D1)	ILA050	C (B)	TAP021	E (E)	TAP067	B (B)
ILA014	D (D3)	ILA053	C (C2)	TAP022	D (D1)	TAP071	B (B)
ILA015	B (B)	ILA054	B (B)	TAP024	D (D1)	TAP075	B (B)
ILA016	D (D2)	ILA055	D (D2)	TAP025	D (D2)	TAP077	B (B)
ILA017	C (D3)	ILA056	D (D2)	TAP026	D (D2)	TAP080	C (B)
ILA018	C (D3)	ILA059	D (D2)	TAP027	D (D2)	TAP084	D (D2)
ILA020	C (C2)	ILA061	C (D3)	TAP031	D (D3)	TAP086	B (B)
ILA026	D (D1)	ILA063	B (B)	TAP032	D (C1)	TAP088	D (B)
ILA027	D (D2)	ILA066	C (D3)	TAP033	C (C2)	TAP089	C (C3)
ILA028	D (D1)	TAP001	E (D1)	TAP035	C (B)	TAP090	D (D3)
ILA029	D (D1)	TAP002	C (C2)	TAP037	D (E)	TAP091	E (D3)
ILA030	D (D1)	TAP003	D (D1)	TAP038	D (D3)	TAP093	D (C2)
ILA031	C (D2)	TAP004	D (E)	TAP039	C (C2)	TAP094	C (B)
ILA032	D (D2)	TAP005	E (E)	TAP040	C (C2)	TAP095	D (D2)
ILA033	D (D2)	TAP006	D (D1)	TAP041	C (C2)	TAP096	E (C1)
ILA034	D (D2)	TAP007	D (E)	TAP043	C (C2)	TAP103	C (B)
ILA035	D (D2)	TAP008	D (E)	TAP044	C (C3)	TAP113	C (B)
ILA036	E (D1)	TAP009	D (D1)	TAP045	B (B)	TAP114	B (C1)
ILA037	D (D1)	TAP010	D (D1)	TAP046	B (C3)		
ILA038	D (D1)	TAP011	D (D1)	TAP051	C (C2)		

Tsai [29] at ILA-DH and TAP-DH. The Err% of the estimated Vs30 are 15.10% and 37.44%, respectively; they are even larger than the LSS at a depth of 15 m (Fig. 3), which has the largest Err% of the three extrapolations (Table 4). Since the largest Err% of BCV at a depth of 15 m are 4.72% and 9.43%, respectively (Table 4), and since most of ILA-SH and TAP-SH have depths of more than 15 m, the estimated Vs30 and site classification of this study are more reliable than those of Lee and Tsai [29] in northeastern Taiwan. Stations in the soil sediments (class E and class D) are located in the Taipei and Ilan basins except for the northernmost one (TAP084); dense soil and firm rock class C is distributed around the basins and along the southern coast line of Ilan; firm to hard rock class B is mostly located in the northeast corner of Taipei.

6. Conclusions

It was found that the influences of soil type and geological epoch are not influential on the relation between Vs, depth, and N in Ilan,

but they are notably significant for that in Taipei. This might be due to the fact that many sites in Taipei are distributed amongst various geological epochs such as Miocene, Pleistocene and Holocene; however, almost all sites in Ilan are located on the Holocene sediments. Multivariable analysis is useful as the data can pass both the rule of the thumb test and stepwise selection to avoid the effect of multicollinearity. Eq. (1) is the preferred regression equation in the Ilan area despite the soil type and geological epoch. Eqs. (2) and (3) are for the Taipei Basin; they can only be employed in the Holocene alluviums, i.e. inside the Taipei Basin based on the soil types. Evidently, Eqs. (1)–(3) can only be applied to the strata less or equal to 50 m because of our data collection.

Three extrapolations were examined in this study by using the borehole data with an actual depth reaching or exceeding 30 m.
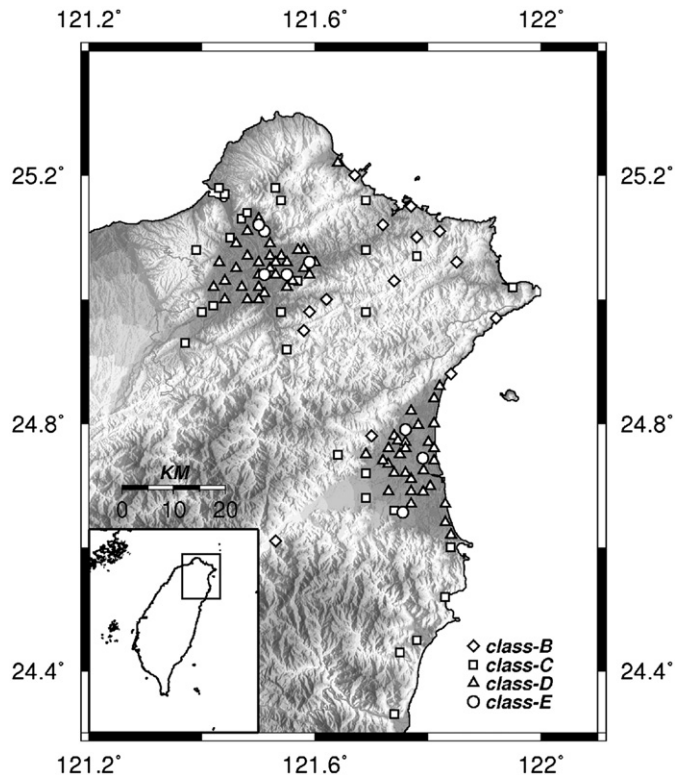
Fig. 7. Distribution of the 110 free-field strong motion stations with boreholes in Ilan and Taipei. They are classified as class B, C, D, and E.

Obviously, BCV is the most accurate and stable extrapolation according to the least Err% and standard deviations (Table 4), although the classified result is identical to that of STS (Table 5). We also found that Boore and Asten [14] extrapolated the bottom velocities to 30 m in their study to compare shear-wave slowness for several models smaller than 30 m. Fig. 6 supports our speculation that the Ss decrease is more slowly in northeastern Taiwan than in California, and this is the reason that BCV is the most suitable extrapolation in northeastern Taiwan. This result brings another interesting phenomenon, namely that the increase of Vs in northeastern Taiwan is more gently than in California at the near surface. Table 6 and Fig. 7 show the classification in northeastern Taiwan according to the $Vs30$ criteria. About one-third of the sites were reclassified (35 of 110 sites) in this study. In addition, the Err% of the estimated $Vs30$ [29] are 15.10% and 37.44% in Ilan and Taipei, respectively. This implies that we must continue constructing reliable site classification and $Vs30$ values in Taiwan by drilling more velocity loggings, and not only estimate them by the relatively low-precision geo-statistical method.

Two approaches (empirical equations and extrapolations) proposed in this study that can be applied at boreholes have only N, and the corresponding depths to calculate the $Vs30$ are less than 30 m, such as DB-151 and SS-B-09. Many existing earlier boreholes can give useful $Vs30$ without additional expense using the proposed approaches.

Acknowledgements

References

[1] Anderson JG, Lee Y, Zeng Y, Day S. Control of strong motion by the upper 30 meters. Bulletin of the Seismological Society of America 1996;86(6): 1749–59.

[2] Dobry R, Borcherdt RD, Crouse CB, Idriss IM, Joyner WB, Martin GR, et al. New site coefficients and site classification system used in recent building seismic code provisions. Earthquake Spectra 2000;16:41–67.

[3] Building Seismic Safety Council (BSSC). NEHRP recommended provisions for seismic regulations for new buildings and other structures, 2000 Edition. Part 1: Provisions, prepared by the Building Seismic Safety Council for the Federal Emergency Management Agency (Report FEMA 368), Washington, DC, 2001.

[4] Massa M, Morasca P, Moratto L, Marzorati S, Costa G, Spallarossa D. Empirical ground-motion prediction equations for northern Italy using weak- and strong-motion amplitudes, frequency content, and duration parameters. Bulletin of the Seismological Society of America 2008;98(3):1319–42.

[5] Power M, Chiou B, Abrahamson N, Bozorgnia Y, Shantz T, Roblee C. An overview of the NGA project. Earthquake Spectra 2008;24(1):3–21.

[6] Chiou B, Darragh R, Gregor N, Silva W. NGA project strong motion database. Earthquake Spectra 2008;24(1):23–44.

[7] Ohta Y, Goto N. Empirical shear wave velocity equations in terms of characteristic soil indexes. Earthquake Engineering and Structural Dynamics 1978;6:167–87.

[8] Lee SHH. Analysis of the multicollinearity of regression equations of shear wave velocities. Soils and Foundations 1992;32(1):205–14.

[9] Chen MH, Wen KL, Loh CH. A study of shear wave velocities for alluvium deposits in southwestern Taiwan. Journal of Chinese Institute of Civil and Hydraulic Engineering 2003;15(4):667–77.

[10] Williams RA, Odum JK, Stephenson WJ, Herrmann RB. Shallow P- and S-wave velocities and site resonances in the St. Louis region, Missouri-Illinois. Earthquake Spectra 2007;23(3):711–26.

[11] Bang ES, Kim DS. Evaluation shear wave velocity profile using SPT based uphole method. Soil Dynamics and Earthquake Engineering 2007;27(8):741–58.

[12] Arai H, Tokimatsu K. Three-dimensional Vs profiling using microtremors in Kushiro, Japan. Earthquake Engineering and Structural Dynamics 2008;37(6): 845–59.

[13] Kuo CH, Cheng DS, Hsieh HH, Chang TM, Chiang HJ, Lin CM, et al. Comparison of three different methods in investigating shallow shear-wave velocity structures in Ilan, Taiwan. Soil Dynamics and Earthquake Engineering 2009;29(1): 133–43.

[14] Boore DM, Asten MW. Comparisons of shear-wave slowness in the Santa Clara Valley, California, using blind interpretations of data from invasive and noninvasive methods. Bulletin of the Seismological Society of America 2008;98(4):1983–2003.

[15] Ohta Y, Goto N. Shear wave velocity measurement during a standard penetration test. Earthquake Engineering and Structural Dynamics 1978;6:43–50.

[16] Boore DM. Estimating $Vs(30)$ (or NEHRP site classes) from shallow velocity models (depths < 30 m). Bulletin of the Seismological Society of America 2004;94(2):591–7.

[17] Boore DM, Joyner WB. Site amplifications for generic rock sites. Bulletin of the Seismological Society of America 1997;87(2):327–41.

[18] Huang MW, Wang JH, Ma KF, Wang CY, Hung JH, Wen KL. Frequency-dependent site amplifications with f≧0.01 Hz evaluated from velocity and density models in central Taiwan. Bulletin of the Seismological Society of America 2007;97(2):624–37.

[19] Wang CY, Lee YH, Ger ML, Chen YL. Investigating subsurface structures and P- and S-wave velocities in the Taipei Basin. Terrestrial Atmospheric and Oceanic Sciences 2004;15(4):609–27.

[20] Chiang SC. A seismic refraction prospecting of the Ilan plain. Mining Technique 1976;14:215–21. (in Chinese).

[21] Hamilton E. Shear wave velocity versus depth in marine sediments: a review. Geophysics 1976;41(5):985–96.

[22] Holzer TL, Bennett MJ, Noce TE, Padovani AC, Tinsley III JC. Shear-wave velocity of surficial geologic sediments: statistical distributions and depth dependence. Earthquake Spectra 2005;21(1):161–77.

[23] Ohsaki Y, Iwasaki R. On dynamic shear moduli and Poisson's ratio of soil deposits. Soils and Foundations 1973;13(4):61–73.

[24] Imai T. P- and S-wave velocities of the ground in Japan. In: Proceedings of the 9th international conference on soil mechanics and foundation engineering, Tokyo, Japan, July 10–15, vol. 2, 1977. p. 257–60.

[25] Seed HB, Idriss IM. Evaluation of liquefaction potential of sand deposits based on observations of performance in previous earthquakes. In: Proceedings of the conference on in situ testing to evaluate liquefaction susceptibility. ASCE; 1981. p. 81–544.

[26] Pitilakis K, Raptakis D, Lontzetidis K, Tika-vassilikou T, Jongmans D. Geotechnical and geophysical description of Euro-seistests, using field and laboratory tests, and moderate strong ground motions. Journal of Earthquake Engineering 1999;3(3):381–409.

[27] Hasancebi N, Ulusay R. Empirical correlations between shear wave velocity and penetration resistance for ground shaking assessments. Bulletin of Engineering Geology and Environment 2007;66:203–13.

[28] Sykora DE, Stokoe KHII. Correlations of in situ measurements in sands of shear wave velocity, soil characteristics and site conditions. Report GR 83-33, Civil Engineering Department, University of Texas at Austin, 1983. 484 pp.

[29] Lee CT, Tsai BR. Mapping Vs30 in Taiwan. Terrestrial, Atmospheric and Oceanic Sciences 2008;19(6):671–82.

[30] Chapman MC, Martin JR, Olgun CG, Beale JN. Site response models for Charleston, South Carolina, and vicinity developed from shallow geotechnical investigations. Bulletin of the Seismological Society of America 2006;96(2):467–89.

[31] Anderson DR, Sweeney DJ, Williams TA. Statistics for business and economics. 2nd ed.. Taipei: West Publishing Company; 1984 668 pp.

[32] Hair Jr. JF, William CB, Barry JB, Rolph EA, Ronald LT. Multivariate data analysis. 6th ed.. Upper Saddle River, NJ: Pearson Education International; 2006 899 pp.

[33] Boore DM. A compendium of P- and S-wave velocities from surface-to-borehole logging: summary and reanalysis of previously published data and analysis of unpublished data. US Geological Survey Open-File Report 03-191, 2003. ⟨http://quake.usgs.gov/~boore⟩.

[34] Holzer TL, Bennett MJ, Noce TE, Padovani AC, Tinsley III JC. Liquefaction hazard and shaking amplification maps of Alameda, Berkeley, Emeryville, Oakland and Piedmont, California: a digital database. US Geological Survey open-file report 02-296, 2002.

[35] Lee CT, Cheng CT, Liao CW, Tsai YB. Site classification of Taiwan free-field strong-motion stations. Bulletin of the Seismological Society of America 2001;91(5):1283–97.

[36] Sokolov VY, Loh CH, Jean WY. Application of horizontal-to-vertical (H/V) Fourier spectral ratio for analysis of site effect on rock (NEHRP-class B) sites in Taiwan. Soil Dynamics and Earthquake Engineering 2007;27(4):314–23.

[37] Kanno T, Narita A, Morikawa N, Fujiwara H, Fukushima Y. A new attenuation relation for strong ground motion in Japan based on recorded data. Bulletin of the Seismological Society of America 2006;96(3):879–97.